ATATÜRK ÜNİVERSİTESİ YAYINLARI
ATATURK UNIVERSITY PUBLICATIONS

Research Article *Araştırma Makalesi* DOI: 10.5281/zenodo.14670892

Numerical Investigation of The Flow in Fractal Type Bifurcation and Trifurcation Systems with Different Features

Farklı Özelliklere Sahip Fraktal Tip Çatallanma ve Üçlükasyon Sistemlerinde Akışın Sayısal İncelenmesi

Ahmet KAHYA
İsak KOTCİOĞLU
Atatürk University, Faculty of Engineering, Mechanical Engineering Erzurum, Türkiye.

ABSTRACT

In this study, CFD and mathematical analyses were performed on straight pipe, double branched and triple branched pipe models. In the straight pipe model, it was observed that the velocity was maximum at the center and decreased towards the wall. While the velocity distribution was homogeneous at the inlet section, the velocity profile changed as the flow developed. In the double branched and triple branched pipe models, it was determined that the velocity decreased in the separation regions and vortex formations caused a decrease in velocity and an increase in pressure. The fact that the side branches were of the same diameter and in the same plane kept the differences in the velocity distribution to a minimum. The results showed that fractal flow systems with small aspect ratios provided less pressure loss.

Keywords: Trifurcation, bifurcation, flow analysis, pressure difference

ÖZ

Bu çalışmada, düz boru, çift çatallı ve üç çatallı boru modelleri üzerinde CFD ve matematiksel analizler gerçekleştirilmiştir. Düz boru modelinde, hızın merkezde maksimum olduğu ve cidara doğru azaldığı gözlemlenmiştir. Giriş kesitinde hız dağılımı homojenken, akış geliştikçe hız profili değişiklik göstermektedir. Çift çatallı ve üç dallı boru modellerinde ise ayrılma bölgelerinde hızın azaldığı, vorteks oluşumlarının hız düşüşüne ve basınç artışına neden olduğu belirlenmiştir. Yan dalların eş çapta ve aynı düzlemde olması, hız dağılımındaki farkları minimal tutmuştur. Sonuçlar, küçük en-boy oranına sahip fraktal akış sistemlerinin daha az basınç kaybı sağladığını göstermiştir.

Anahtar Kelimeler: Trifurkasyon, bifurkasyon, akış analizi, basınç farkı

Received/Geliş Tarihi: 06.12.2024
Accepted/Kabul Tarihi: 06.01.2025
Publication Date/Yayın Tarihi: 17.01.2025

Corresponding Author/Sorumlu Yazar:
Ahmet KAHYA
E-mail: ahmet.kahya14@atauni.edu.tr

Cite this article: Kahya A., Kotcioğlu İ., (2024), Numerical Investigation of The Flow in Fractal Type Bifurcation and Trifurcation Systems with Different Features. *Journal of Energy Trends*, 1(2), 47-58

Introduction

In various engineering applications, fractal-like geometric structures, new ideas, namely flow systems and approaches representing similar small-scale structures, have theoretically shaped the basic ideas of the research field in general over the past quarter century. This idea was inspired by living and non-living objects and is important for the future of applied engineering. In sequential and multi-flow systems with such similar structures, it is important to distribute the single-phase fluid evenly throughout the channel (Bejan, 1997). These channels can have symmetrical (regular) and asymmetrical (irregular) structures. As in circulatory systems, the branches or bifurcations in multi-flow systems can have narrowing and widening structures.

The mathematical behaviors and models of such physical mechanisms are similar to each other (Senn & Poulikakos, 2004). Fundamental laws such as Poiseuille and continuity equations in terms of fluid mechanics, Ohm's law for electrical circuits, Fourier equation in heat transfer calculations, Murray's law for bifurcation or fractal structures in biological systems are mathematically similar to each other.

In order to obtain the best heat transfer performance of fractal-like channel networks, optimization of many geometric factors is required. Examples of these geometric factors are; number of levels (L), number of branches-number of bifurcations (n), bifurcation angle (θ), length scale ratio (γ), width scale ratio (β), and terminal (end boundary) channel width (w_m). To find the optimum point by establishing a relationship between these factors and to ensure that the system to be created is more efficient (Alharbi et al. 2003).

1. Theoretical Foundations

Bifurcation or branching is a phenomenon frequently seen in multi-flow systems. At these points, we can encounter expanding or contracting structures, they can be symmetrical or asymmetrical. Comparison of such structures with Newtonian and non-Newtonian fluids with different flow conditions is of great importance for various application areas. For example, they can be seen in many physical mechanisms, from biological systems such as blood vessels or lung airways to city water networks. They are also important in many areas, from cooling systems of electronic circuits to the development of new generation heat exchangers. Analogies of such systems can lead to important advances in different areas (Kotcioğlu, 2017).

1.1. Constructal Theory

Constructal theory is an approach that explains how complex structures consisting of many interconnected simple elements are formed in nature. This theory suggests that systems in nature adapt to perform their functions with the least energy expenditure. Using reverse engineering methods, the properties of these optimized structures in nature are examined and practical applications of this information are developed. Constructal theory can be observed in many areas from biological organisms to streams, from heat transfer to electric current. This theory helps us understand the complexity of nature and find more efficient and sustainable solutions in technology (Wang et al. 2010a).

2. Fractal, Bifurcation and Branch Geometry

2.1. Fractal (leaf) Structure

They are geometric shapes that are mathematically defined and have self-similarity. These shapes repeat the same structure at any scale. They have repeating building blocks that form a certain pattern, and these building blocks create a smaller copy of the same pattern at each scale. Fractals are used in modeling complex structures frequently observed in nature. Structures such as leaves, butterfly wings, circulatory systems, tree branches are examples of these structures (Colak et al. 2018).

2.2. Bifurcation Structure

Another structure similar to fractal structures is bifurcation (double branch) structures. Bifurcation is the occurrence of two or more different states or behaviors in a system after a certain point. Generally, in mathematical and physical systems, the values of variables change suddenly after a certain critical point, leading to new and different behaviors (Blonski et al. 2020). They can be designed according to applications in various engineering fields in a regular structure and in the form of elastic veins. These designed structures are models that have become increasingly important in terms of engineering applications. Symmetrical and asymmetrical structures are shown in Figure 1.

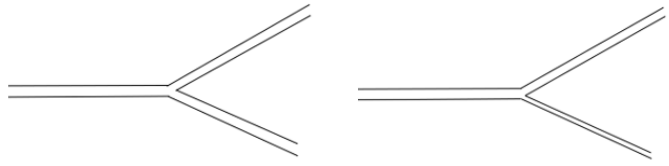

Figure 1.
Symmetrical (bifurcation), Non-symmetrical (bifurcation) structures

2.3. Branch Structure

A complex structure similar to fractal structures; these structures are models that contain fractal and bifurcation structures together (Muwanga et al. 2008). They are structures that include structures such as leaf, butterfly wing, dill, etc. as well as vein, network systems, tree branches, etc. Different branch structures are shown in Figure 2. They are also created in a certain hierarchical order.

3. Mathematical Model

The Navier-Stokes equations for a cylindrical pipe (vessel) are given below. The flow velocity vector is defined as vectorial ($\vec{U}$) by the following 1 equation.

$$\vec{U} = u(ue_r + ve_\phi + we_z) \quad (1)$$

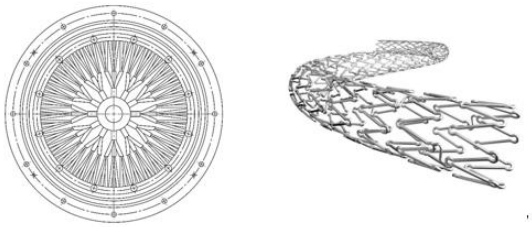

(a) (b)

Figure 2.
a) Disc-shaped flow tube, b) Vascular stent (Çolak, 2017)

From the equation, for one-dimensional axial flow in cylindrical pipes, $u = u(r)$ is a function of u. The other fluid velocities in both directions are $v = w = o$ and → ∂/∂z = 0. Here, the continuity equation for three-dimensional and one-dimensional flow in cylindrical coordinates is given by the following equation in vectorial and differential form (Equation 2).

$$\vec{\nabla}.\vec{V} = \frac{1}{r}\left[r\frac{\partial u}{\partial r} + r\frac{\partial v}{\partial \phi} + \frac{\partial w}{\partial z}\right] \quad (2)$$

The same equation is given below for one-dimensional ($v = w = o$) flow (Equation 3).

$$\vec{\nabla}.\vec{V} = \frac{1}{r}\left[r\frac{\partial u}{\partial r}\right] = 0 \rightarrow u \neq f_n(x) \rightarrow u = u(r) \quad (3)$$

The momentum equation is expressed in vector form in the following equation (Equation 4).

$$\rho[\frac{\partial \vec{V}}{\partial t} + \vec{U}.\vec{\nabla}\vec{U}] = -\vec{\nabla}P + \rho\vec{g} + \mu\vec{\nabla}^2\vec{U} = \frac{1}{r}(r\frac{\partial^2 u}{\partial r^2})\,\vec{e}_r \quad (4)$$

In this equation,$\vec{\nabla}P$ is the pressure gradient. In equation (5), the dimensionless number Reynolds number, which determines the flow regime of the fluid passing through the channel, is given by the following equation.

$$Re = \frac{\rho.D_h.U}{\mu} \quad (5)$$

In this equation,D_h is the hydraulic diameter, ρ is the density, U is the velocity, μ is the dynamic viscosity. The wall shear stress in a straight cylindrical pipe (vessel) in steady laminar flow is defined by the following equation (Equation 6).

$$\tau_\omega = \frac{32\mu\dot{Q}}{\pi r^3} \quad (6)$$

$\dot{Q}$ given in the equation is the volumetric flow rate. The equation of the velocity distribution in a cylindrical pipe in steady flow is defined by the following 7 equation.

$$u = U_{max}\,(1 - \frac{r^2}{R^2}) \quad (7)$$

The velocity distribution in pulsatile flow is expressed by the following 8 equation.

$$u = U_{max}(1 + sin(2\pi.t)) \quad (8)$$

According to Poiseuille's law, the volumetric flow rate of a fluid passing through a cylindrical pipe in steady flow is given by the following 9 equation.

$$\dot{Q} = \Delta P.\pi.\frac{r_i^4}{8\mu} \quad (9)$$

In this equation, ΔP is the pressure difference between the inlet and outlet. The wall shear stress is defined according to the volumetric flow rate and pressure difference as given below, respectively (Equation 10).

$$\tau = \frac{4\mu\dot{Q}}{\pi r_i^3} \quad (10)$$

3.1 Murray's Law

Murray's law is a principle proposed to optimize efficiency by minimizing the required blood (fluid) flow and energy in a vessel (branch-pipe) (Lee, J. Y. & Lee, S. J. 2010). In its simplest form, the equation for a parent vessel with a radius r_0 and two daughter branches with radii r_1 and r_2 is given by the Equation (11).

$$r_0^\lambda = r_1^\lambda + r_2^\lambda \quad (11)$$

In this equation, r0 is the radius of the main branch, while r1 and r2 are the radii of the side branches. λ represents the branching exponent. According to Murray's law, when λ=3 it indicates that the flow energy is minimized. For this reason, λ=3 is typically used in the formula. Accordingly, Equation (12) becomes:

$$r_0^3 = r_1^3 + r_2^3 \quad (12)$$

is arranged as follows.

4.Fluid (Water) Properties

The properties of the fluid used in the analysis are given in Table 1.

Table 1.
Density and viscosity of fluids

Newtonian	**μ (kgm^{-1}s^{-1})**	**P (kgm^{-3})**
Newtonian (Water)	0.008	997

5. RESULTS AND DISCUSSION

In this study, various solid models, including straight pipe (Figure 3), bifurcation pipe (Figure 10), and trifurcation pipe (Figure 17), were designed using the SolidWorks software in accordance with the specifications provided in the tables (2-4). Velocity and pressure analyses were then performed on these models using ANSYS software. Subsequently, the analysis results were supported and evaluated using MATLAB (Figure 24-25) software.

5.1. Straight Pipe Ansys Analysis

The properties of straight pipes analyzed with Ansys were drawn with the SolidWorks program according to the data in Table 2.

Table 2.
Characteristics of the pipe

Pipe	Diameter(mm)	Length(mm)
1	6	70
2	8	80
3	10	90

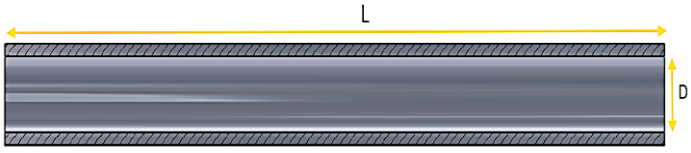

Figure 3.
Straight pipe cross-sectional area

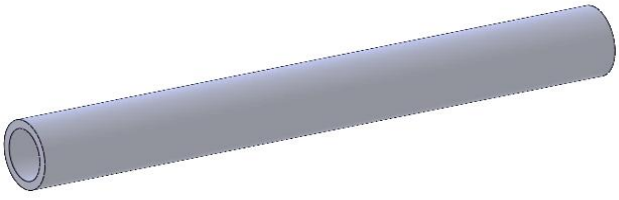

Figure 4.
Straight pipe (D=6mm, L=70mm)

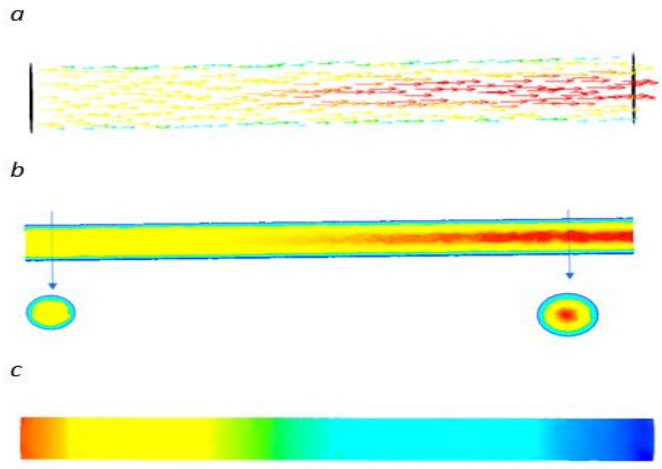

Figure 5.
a) Ansys vector velocity analysis for straight pipe (D=6mm, L=70mm), b) Ansys velocity analysis for straight pipe, c) Ansys pressure analysis for straight pipe (D=6mm, L=70mm)

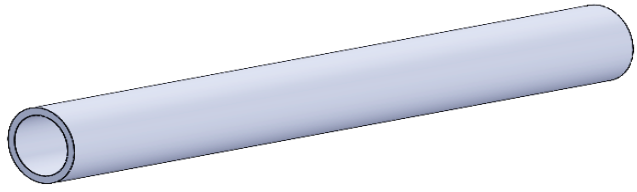

Figure 6.
Straight pipe (D=8mm, L=80mm)

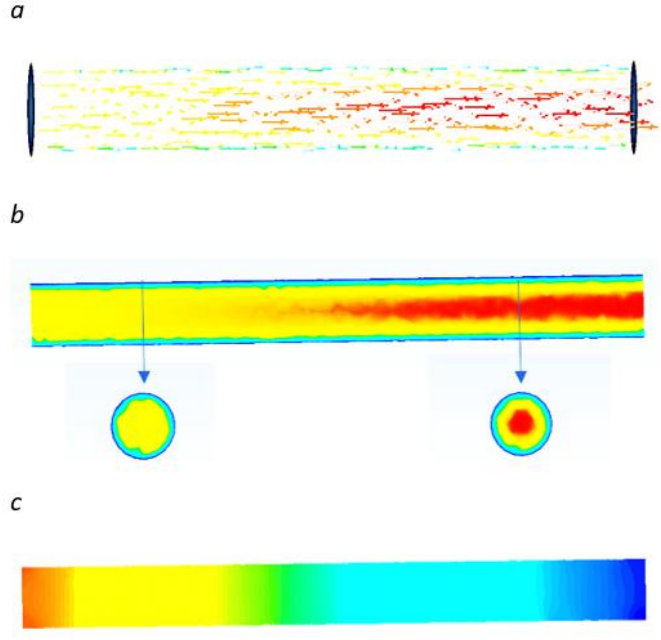

Figure 7.
a) Ansys vector velocity analysis for straight pipe (D=8mm, L=80mm), b) Ansys velocity analysis for straight pipe (D=8mm, L=80mm), c) Ansys pressure analysis for straight pipe (D=8mm, L=80mm)

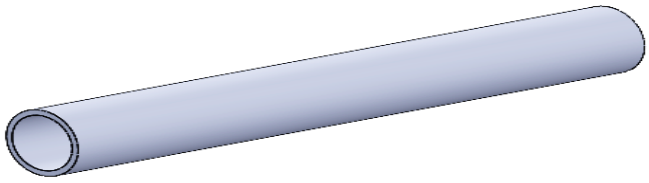

Figure 8.
Straight pipe (D=10mm, L=90mm)

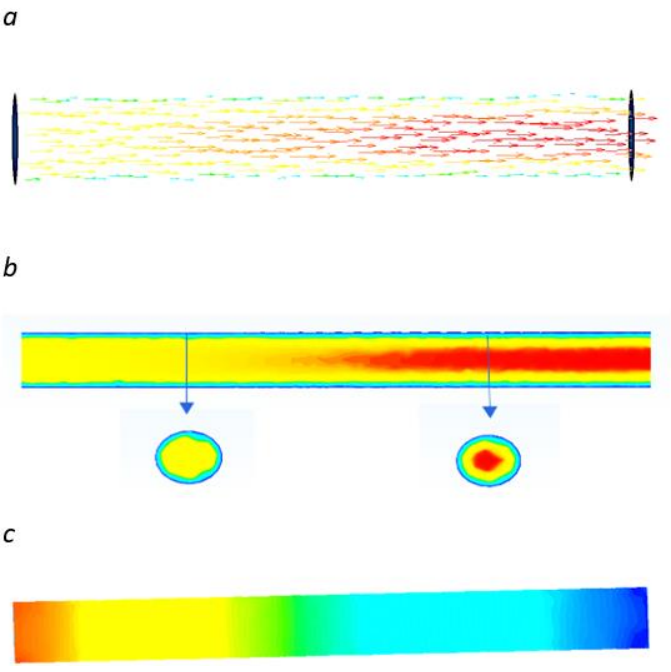

Figure 9.
a) Ansys vector velocity analysis for straight pipe (D=10mm, L=90mm), b) Ansys velocity analysis for straight pipe (D=10mm, L=90mm), c) Ansys pressure analysis for straight pipe (D=10mm, L=90mm)

The flow of water at a velocity of 0.3 m/s through a straight pipe with a diameter of 6 mm and a length of 70 mm was analyzed using ANSYS. The physical dimensions of the pipe are shown in Figure 4. According to the velocity analysis results, the velocity distribution of the water inside the pipe is represented by a color scale. As shown in Figure 5-a with vector lines and Figure 5-b, the highest velocity was observed at the center of the pipe, while it decreased toward the edges. This indicates a velocity profile consistent with laminar flow characteristics. In the vector velocity analysis, local velocity variations along the pipe were observed, where higher velocity regions are represented by red and yellow colors, while lower velocity regions are represented by blue colors. The pressure analysis revealed a pressure drop from the inlet to the outlet of the pipe. As illustrated in Figure 5-c, the color scale indicates a transition from high pressure to low pressure, which is a result of frictional losses along the pipe during the flow. The flow of water at a velocity of 0.3 m/s through a straight pipe with a diameter of 8 mm and a length of 80 mm was also analyzed. The physical dimensions of this pipe are shown in Figure 6. According to the velocity analysis results, the velocity distribution of the water inside the pipe is represented by a color scale. As shown in Figures 7-a and Figure 7-b, the highest velocity was observed at the center of the pipe, while it decreased toward the edges. This is consistent with the characteristics of laminar flow. In the vector velocity analysis, local velocity variations along the pipe were observed, where higher velocity regions are represented by red and yellow colors, while lower velocity regions are represented by blue colors. The pressure analysis revealed a pressure drop from the inlet to the outlet of the pipe. As illustrated in Figure 7-c, the color scale indicates a transition from high pressure to low pressure, which is a result of frictional losses along the pipe during the flow. The flow of water at a velocity of 0.3 m/s through a straight pipe with a diameter of 10 mm and a length of 90 mm was also analyzed. The physical structure of the pipe is visually presented in Figure 8. According to the flow analysis, the velocity distribution of the water inside the pipe is notably higher at the center and lower toward the edges. As shown in Figure 9-a, the vector velocity analysis details the velocity variations along the pipe, with high-velocity regions represented by red and yellow tones at the center and low-velocity regions represented by blue tones toward the edges. This demonstrates the laminar nature of the flow. The velocity analysis results presented in Figure 9-b provide a broader perspective on the overall velocity profile of the water inside the pipe. It was observed that the water moves faster at the center of the pipe, while the velocity decreases at the edges due to friction. Pressure analysis results showed a pressure drop from the inlet to the outlet of the pipe. As depicted in Figure 9-c, the color scale clearly shows a transition from high pressure (red) to low pressure (blue). This pressure drop is evaluated as a natural result of frictional effects along the pipe. In the comparison of the pipes in terms of their diameters and lengths, it was observed that as the diameter increased, the velocity profile became more homogeneous, and pressure loss decreased. In the pipe with a 6 mm diameter, due to the narrow cross-section, the velocity was concentrated at the center and decreased significantly towards the edges. This pipe experienced the highest-pressure loss. In the pipe with an 8 mm diameter, the velocity profile was more balanced, with a smoother transition in velocity reduction at the edges. In the pipe with a 10 mm diameter, the velocity distribution was the most homogeneous, with a very slight decrease in velocity from the center towards the edges. Moreover, this pipe exhibited the lowest pressure loss among the three. In terms of length, as the pipe length increased, frictional pressure losses also increased. In the 70 mm long pipe, the pressure loss was limited due to the short distance; however, the narrow diameter made friction losses more pronounced. In the 80 mm long pipe, frictional

effects became more apparent, but the velocity distribution remained relatively balanced. In the 90 mm long pipe, the highest frictional losses occurred; however, the wider diameter mitigated the impact of these losses on the flow, resulting in a more balanced velocity profile.

Overall, pipes with larger diameters and shorter lengths offered lower pressure losses and more homogeneous velocity profiles, providing more efficient flow characteristics. As the diameter increased, the velocity distribution became more uniform, while increased length led to higher frictional losses. Considering these two factors together is essential for optimizing flow performance.

5.2. Ansys Analysis for Bifurcation Pipe

The properties of bifurcation pipes analyzed with Ansys were drawn with the SolidWorks program according to the data in Table 3.

Table 3.
Characteristics of the pipe

Pipe	1.Diameter (mm)	2.Diameter (mm)	Main Pipe length (mm)	Side Pipe length (mm)	Angle
1	6	4	70	50	50
2	8	6	80	60	60
3	10	8	90	70	70

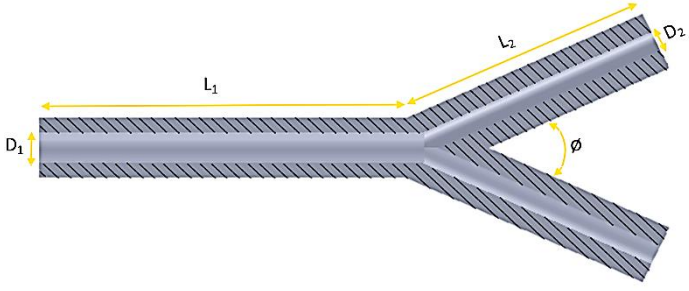

Figure 10.
Bifurcation pipe cross-sectional area

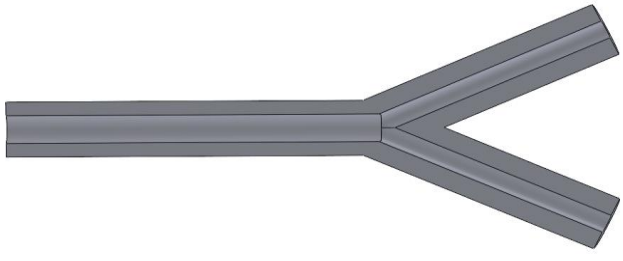

Figure 11.
Bifurcation pipe (D_1=6mm, D_2=4mm, L_1=70mm, L_2=50, Ø=50°)

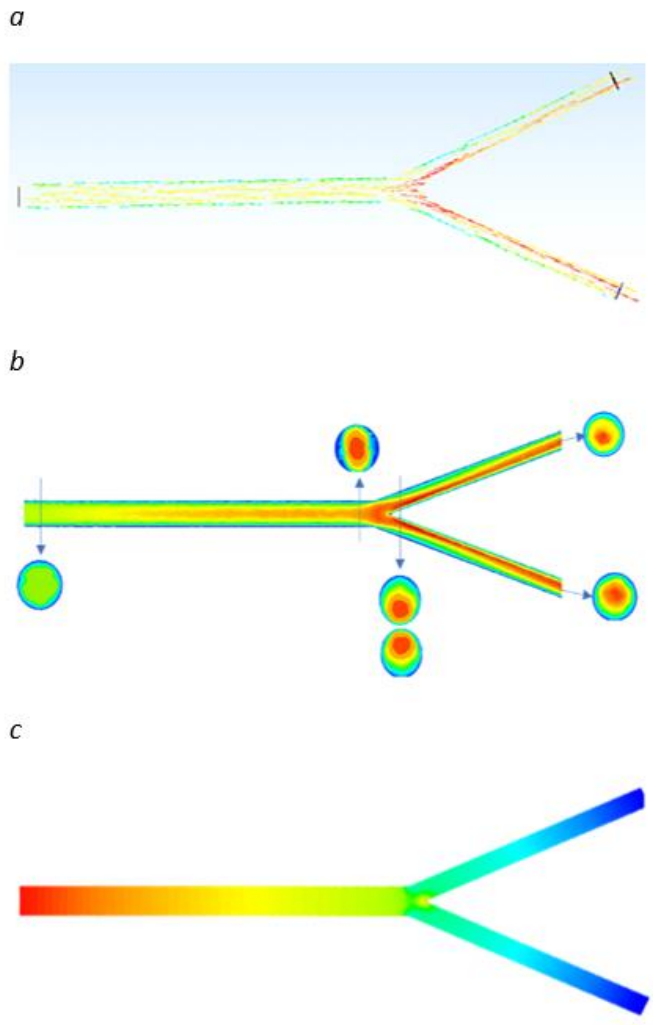

Figure 12.
a) Ansys vector velocity analysis for bifurcation pipe, b) Ansys velocity analysis for bifurcation pipe (D1=6mm, D2=4mm, L1=70mm, L2=50, ø=50°), c) Ansys pressure analysis for bifurcation pipe (D1=6mm, D2=4mm, L1=70mm, L2=50, ø=50°)

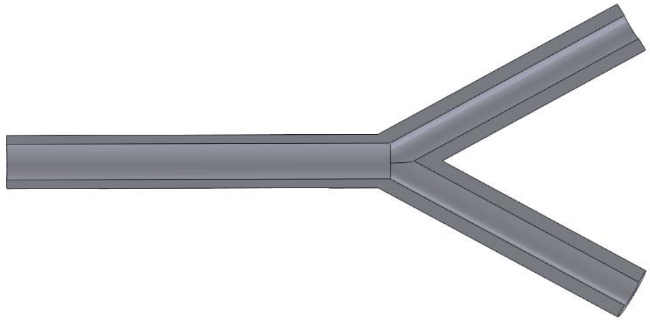

Figure 13.
Bifurcation pipe (D_1=8mm, D_2=6mm, L_1=80mm, L_2=60, Ø=60°)

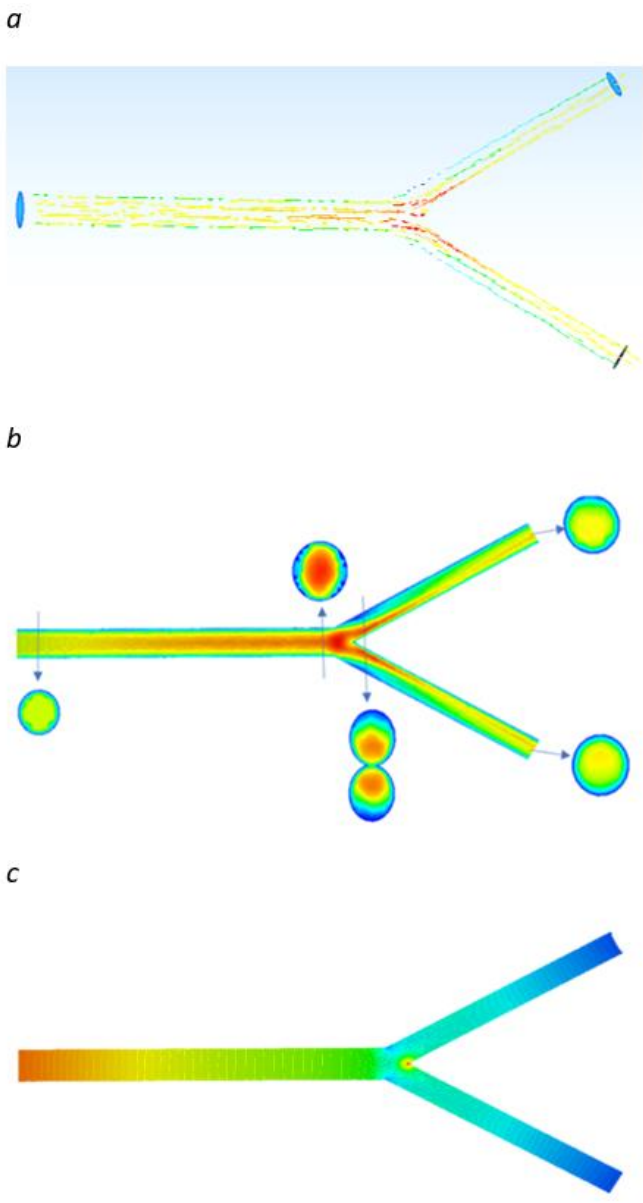

Figure 14.
a) Ansys vector velocity analysis for bifurcation pipe, b) Ansys velocity analysis for bifurcation pipe (D1=8mm, D2=6mm, L1=80mm, L2=60, ø=60°), c) Ansys pressure analysis for bifurcation pipe (D1=8mm, D2=6mm, L1=80mm, L2=60, ø=60°)

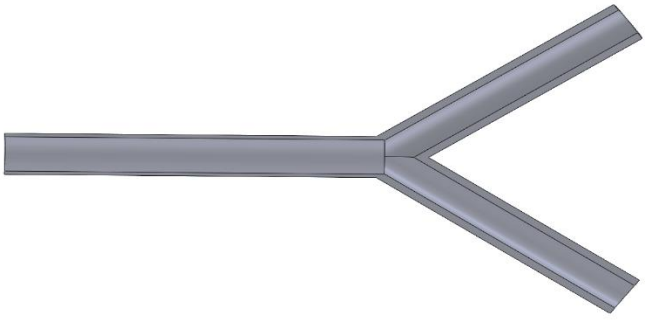

Figure 15.
Bifurcation pipe (D1=10mm, D2=8mm, L1=90mm, L2=70, ø=70°)

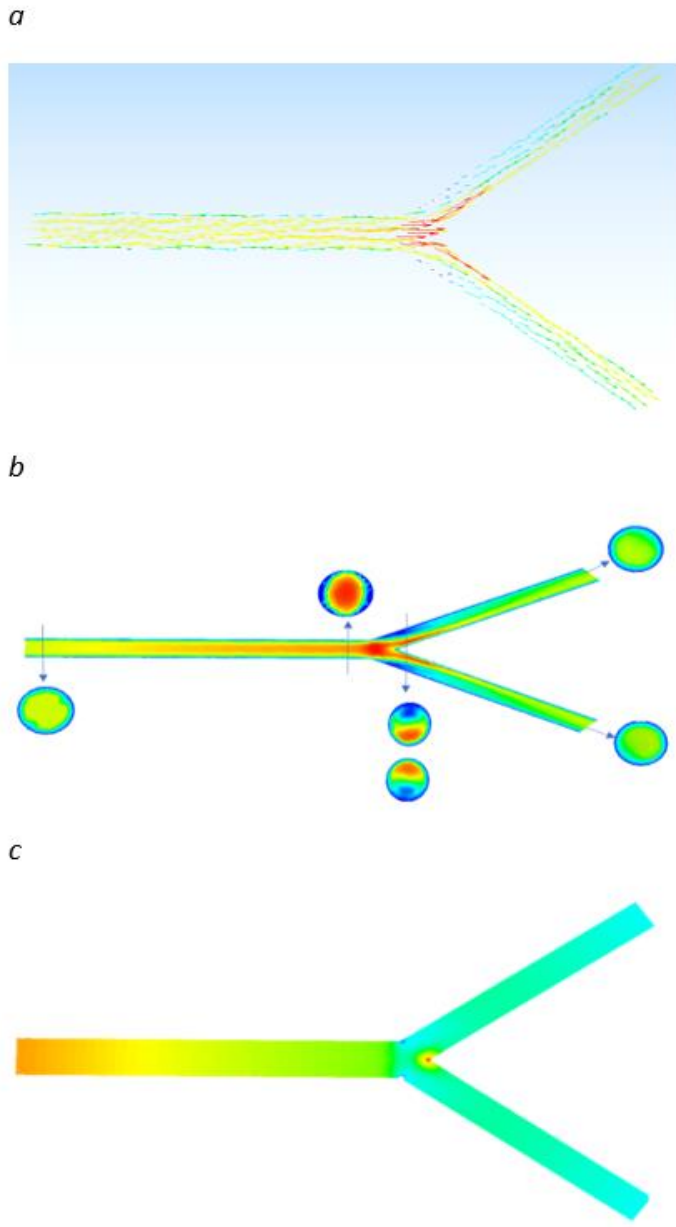

Figure 16.
a) Ansys vector velocity analysis for bifurcation pipe, b) Ansys velocity analysis for bifurcation pipe, c) Ansys pressure analysis for bifurcation pipe

The flow of water at a velocity of 0.3 m/s through a pipe with an inlet diameter of D_1=6 mm, outlet diameters of D_2=4 mm, inlet length of L_1=70 mm, outlet lengths of L_2=50 mm, and bifurcation angle of ø=50° was analyzed using Ansys. The physical dimensions of the pipe are shown in Figure 11. The velocity analysis results Figures 12-a and Figure 12-b illustrate the velocity distribution of the water inside the pipe using a color scale. A significant decrease in velocity was observed at the bifurcation point due to the directional change in the flow and the angular structure of the pipe. The velocity profile indicates that the highest velocities occur in the inlet region and decrease along the branches. Additionally, the 50° angle increased the

turbulence level during flow direction change and caused local velocity differences around the bifurcation point. These differences are represented by red and yellow colors for high-velocity regions and blue colors for low-velocity regions. The vectorial analysis in Figure 12-a shows the directional components of the flow. According to the analysis results, the 50° angle intensified the flow direction change at the bifurcation point and increased the turbulence in this region. Due to the turbulence, the flow did not distribute uniformly along the branches, and higher velocities were observed in some areas. The pressure analysis is shown in Figure 12-c. The results indicate a pressure drop from the inlet to the outlets of the pipe. This pressure drop is depicted using a color scale transitioning from red to blue, reflecting the flow direction change and friction losses caused by the 50° angle. The magnitude of the angle led to fluctuations in both velocity and pressure, resulting in an uneven pressure distribution at the outlets. The geometric properties of another bifurcation pipe are shown in Figure 13, where the pipe has an inlet diameter of D_1=8 mm, outlet diameter of D_2=6 mm, inlet length of L_1=80 mm, outlet lengths of L_2=60 mm, and bifurcation angle of ø=60°. This design allows for a directional flow change and provides the means to analyze velocity and pressure profiles. The vectorial velocity distribution of the flow, illustrated in Figure 14-a, demonstrates the directional and magnitude components of the water velocity inside the pipe using colored vectors. Higher velocities were observed in the inlet region, while reductions in velocity occurred at the bifurcation point due to the directional change. Additionally, the bifurcation angle increased turbulence, causing the flow to distribute unevenly along the branches. The velocity distribution within the pipe, represented by a color scale in Figure 14-b, highlights high-velocity regions in red and yellow tones, while blue and green tones indicate low-velocity regions. The analysis shows that maximum velocity occurs in the inlet region, and a significant decrease is evident at the bifurcation point. The 60° bifurcation angle intensified local velocity differences and turbulence, with a gradual decrease in velocity along the branches. The pressure distribution of the pipe is depicted in Figure 14-c using a color scale transitioning from red to blue. The results reveal high pressure in the inlet region, with a notable decrease at the bifurcation point and along the branches. This outcome is attributed to friction losses and the directional change of the flow. The 60° angle caused pressure fluctuations and resulted in an uneven pressure distribution at the outlets. The geometric properties of a third bifurcation pipe are shown in Figure 15. The pipe has an inlet diameter of D_1=10 mm, outlet diameter of D_2=8 mm, inlet length of L_1=90 mm, outlet lengths of L_2=70 mm, and a bifurcation angle of ø=70°. This design facilitates flow direction changes and provides a detailed investigation of velocity and pressure profiles. The vectorial velocity analysis presented in Figure 16-a shows the directional and magnitude components of the water velocity using colored vectors. High velocities were observed in the inlet region, while reductions in velocity occurred at the bifurcation point due to directional changes. Additionally, the 70° bifurcation angle increased turbulence, leading to uneven flow distribution along the branches. Local velocity differences were also observed due to the turbulence. The velocity distribution represented in Figure 16-b uses a color scale to highlight high-velocity regions in red and yellow tones, while blue and green tones indicate low-velocity regions. The analysis confirms maximum velocity at the inlet, with a significant reduction in velocity at the bifurcation point. The 70° bifurcation angle contributed to turbulence-induced irregularities in the velocity profile, with a gradual reduction in velocity along the branches. The pressure distribution of the pipe is illustrated in Figure 16-c, where a transition from red to blue indicates a pressure drop from the inlet to the outlets. High pressure is evident in the inlet region, with a decrease at the bifurcation point and along the branches. The 70° angle caused fluctuations in pressure due to the flow direction change and friction losses, resulting in an uneven pressure profile at the outlets.

5.3. Ansys Analysis for Trifurcation Pipe

The properties of trifurcation pipes analyzed with Ansys were drawn with the SolidWorks program according to the data in Table 4.

Table 4.
Characteristics of the pipe

Pipe	1.Diameter (mm)	2.Diameter (mm)	Main Pipe length (mm)	Side Pipe length (mm)	Angle
1	6	4	70	50	50
2	8	6	80	60	60
3	10	8	90	70	70

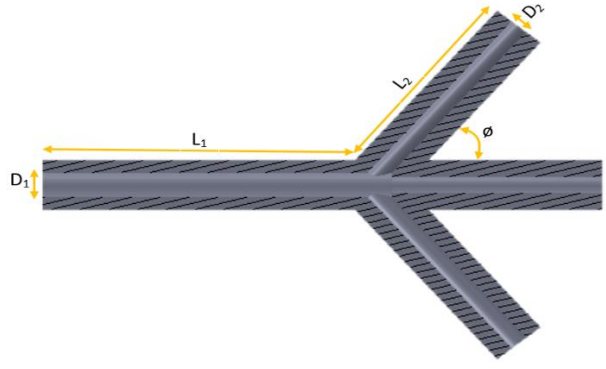

Figure 17.
Trifurcation pipe cross-sectional area

a

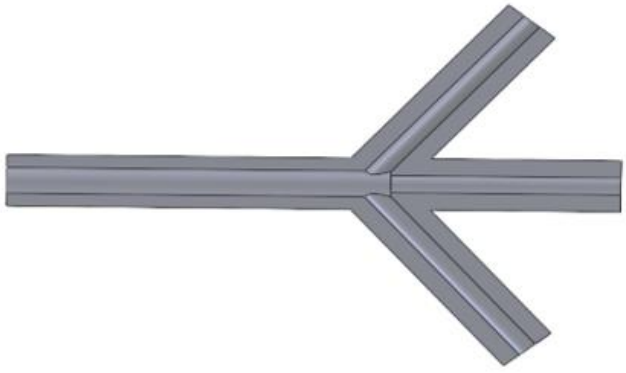

b

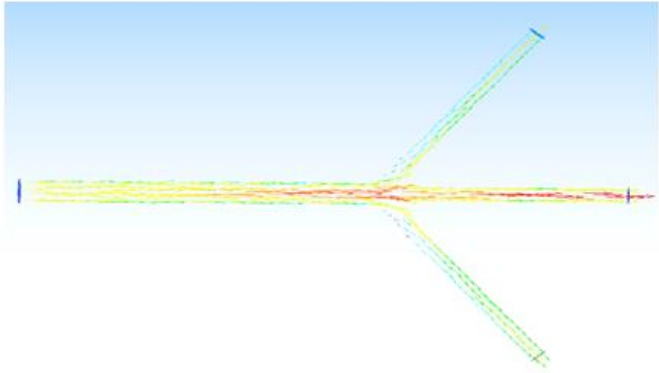

Figure 18.
a) Trifurcation pipe (D1=6mm, D2=4mm, L1=70mm, L2=50, ø=50°), b) Ansys vector velocity analysis for trifurcation pipe

a

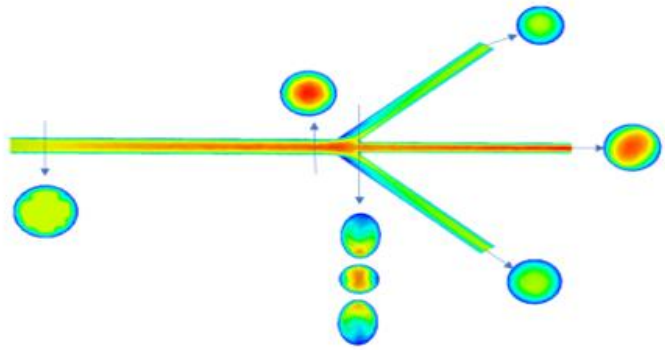

b

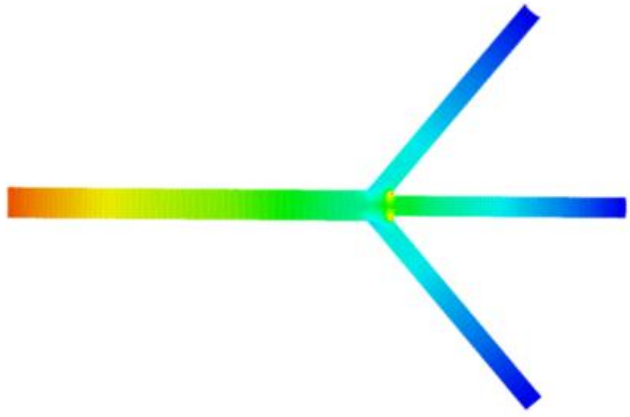

Figure 19.
a) Ansys velocity analysis for trifurcation pipe, b) Ansys pressure analysis for trfurcation pipe

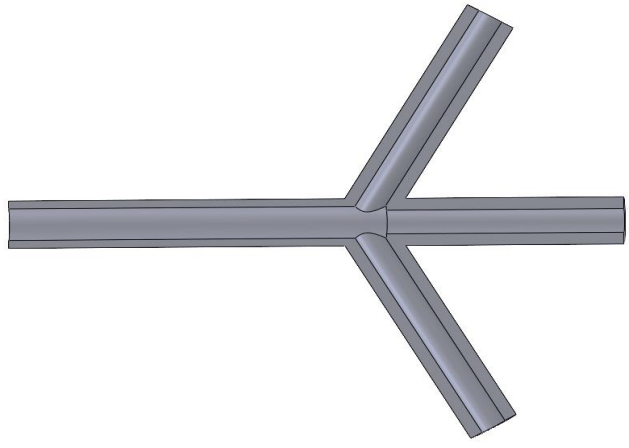

Figure 20.
Trifurcation pipe (D1=8mm, D2=6mm, L1=80mm, L2=60, ø=60°)

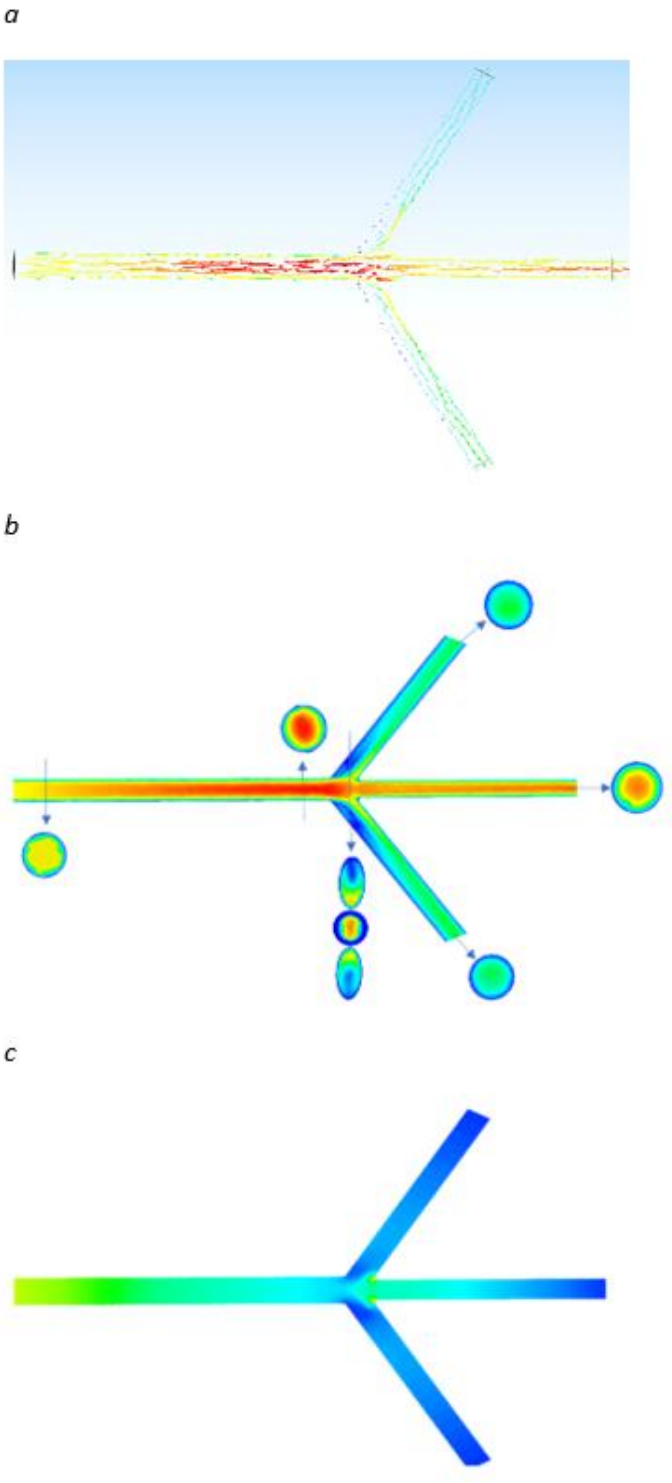

Figure 21.
a) Ansys vector velocity analysis for trifurcation pipe, b) Ansys velocity analysis for trifurcation pipe, c) Ansys pressure analysis for trifurcation pipe

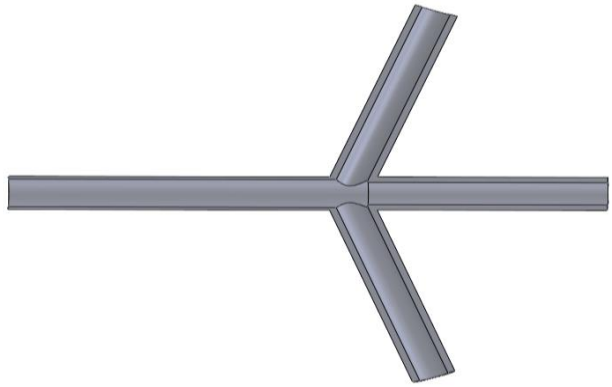

Figure 22.
Trifurcation pipe (D_1=10mm, D_2=8mm, L_1=90mm, L_2=70, Ø=70°)

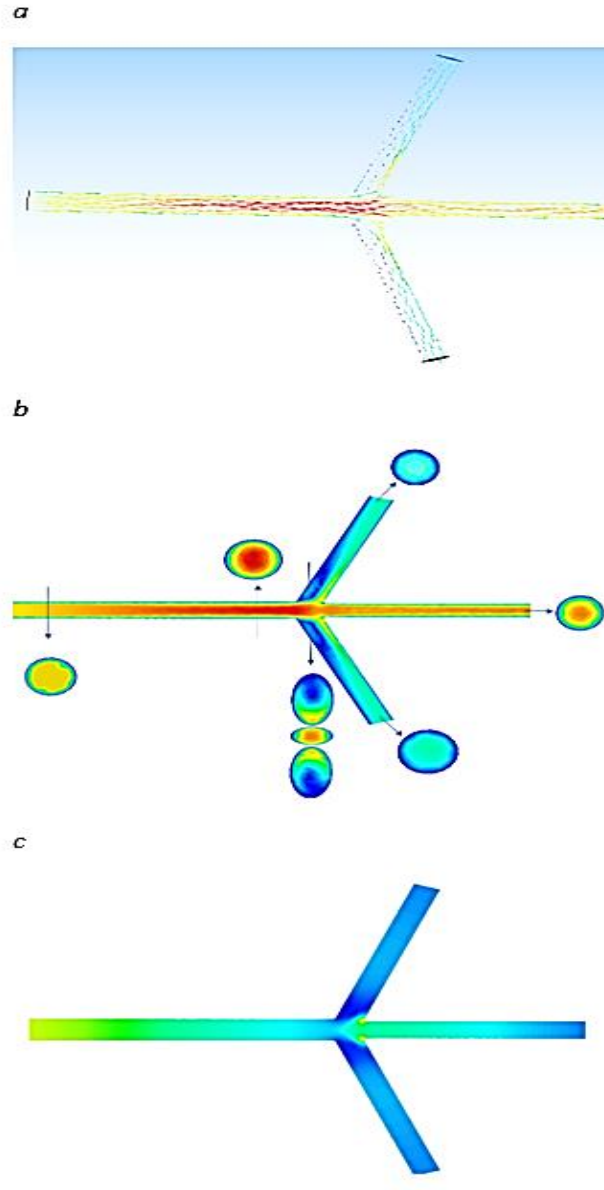

Figure 23.
a) Ansys vector velocity analysis for trifurcation pipe, b) Ansys velocity analysis for trifurcation pipe, c) Ansys pressure analysis for trifurcation pipe

The design and analysis results of the trifurcation pipe have been explained in detail. Figure 17 and Figure 18-a illustrates the geometric properties of the trifurcation pipe. According to this design, the inlet diameter is D_1=6 mm the outlet diameter is D_2=4 mm, the inlet pipe length is L_1=70 mm, the outlet pipe length is L_2=50 mm, and the angle between the pipes is Ø=50°.These dimensions are fundamental parameters used in fluid dynamics analyses. The velocity vectors within the trifurcation pipe were analyzed using ANSYS software, as shown in Figure 18-b. The distribution of velocity vectors demonstrates how the fluid is directed from the inlet towards the branches. This analysis was conducted to examine the impact of the trifurcation pipe design on flow performance. The direction and intensity of the vectors clearly reveal the effect of the pipe geometry on the flow. The results of the velocity analysis are detailed in Figure 19-a. The color scale represents the velocity values of the fluid. According to the analysis, the velocity is higher at the inlet of the pipe and changes as it progresses towards the branches. This velocity distribution indicates that the fluid is effectively divided into the branches in accordance with the pipe design, confirming the design's ability to guide the fluid. The pressure analysis is presented in Figure 19-b. In this analysis, high-pressure values were observed at the inlet of the trifurcation pipe, while the pressure gradually decreased across the branches. The color distribution clearly demonstrates the pressure drop from the inlet to the outlets. This phenomenon highlights the energy loss and redistribution effect occurring during the division of the fluid into the branches. Figure 20 illustrates the geometric properties of the trifurcation pipe. In this design, the inlet diameter is D_1=8 mm, the outlet diameter is D_2=6 mm, the inlet pipe length is L_1=80 mm, and the outlet pipe length is L_2=60 mm. The angle between the branches is Ø=60°. These geometric parameters serve as the basis for fluid dynamics analyses conducted in subsequent steps. The velocity vectors inside the trifurcation pipe are analyzed and visualized in Figure 21-a using ANSYS software. The vector plot demonstrates the flow distribution and directional behavior of the fluid as it enters the pipe and branches out. The vectors highlight the influence of the pipe's geometry on the flow, showing how the fluid transitions and adjusts within the bifurcated structure. Figure 21-b presents the results of the velocity distribution analysis. The color scale in the figure represents the fluid velocity, with higher values concentrated at the inlet and a gradual reduction as the flow progresses into the branches. This velocity distribution indicates the efficiency of the pipe design in directing and distributing the fluid evenly across its outlets. The pressure distribution analysis is shown in Figure 21-c. The results reveal high-pressure regions at the pipe's inlet, with a consistent pressure drop as the fluid moves through the pipe and into the branches. The color scale in the figure clearly visualizes this gradient, emphasizing the energy dissipation and redistribution effects occurring during the flow division process. Figure 22 illustrates the geometric properties of the trifurcation pipe. In this design, the inlet diameter is D_1=10 mm, the outlet diameter is D_2=3 mm, the inlet pipe length is L_1=90 mm and the outlet pipe length are L_2=70 mm. The angle between the pipes is Ø=70°.These measurements form the basis for the fluid dynamics analysis conducted on the pipe. Figure 23-a shows the velocity vectors within the trifurcation pipe, analyzed using ANSYS software. The velocity vectors visualize how the fluid is directed from the inlet toward the branches. The density and direction of the vectors highlight the flow distribution and behavior within the pipe based on its design. This analysis aims to evaluate the pipe's effectiveness in directing fluid flow. The velocity distribution analysis results are presented in Figure 23-b. The color scale represents the velocity values within the pipe. According to the analysis, the velocity is higher at the inlet and decreases significantly as the fluid progresses toward the branches. This indicates that the fluid is effectively divided among the branches in line with the pipe's geometry, demonstrating the design's efficiency in controlling flow. Figure 23-c presents the pressure analysis results. The analysis shows high pressure at the inlet, with a gradual decrease across the branches. The color scale clearly illustrates the pressure loss and redistribution as the fluid divides into the branches.

6. Solutions with the help of Matlab

```
% Kullanıcıdan Girdi Alma
D = input('Boru çapını girin (m): ');            % Boru çapı (m)
L = input('Boru uzunluğunu girin (m): ');        % Boru uzunluğu (m)
u_avg = input('Ortalama hızı girin (m/s): ');    % Ortalama hız (m/s)
rho = input('Su yoğunluğunu girin (kg/m^3): ');  % Su yoğunluğu (kg/m^3)
mu = input('Su dinamik viskozitesini girin (Pa·s): ');% Su viskozitesi

% Hesaplamalar
R = D / 2;                  % Borunun yarıçapı (m)

% 1. Reynolds Sayısı Hesabı
Re = (rho * u_avg * D) / mu;
fprintf('\nReynolds Sayısı: %.2f\n', Re);

% 2. Darcy-Weisbach Basınç Düşüşü
if Re < 2300
    f = 64 / Re;            % Laminer akış için sürtünme katsayısı
else
    f = 0.079 * Re^(-0.25); % Türbülanslı akış için sürtünme katsayısı
end
Delta_p = f * (L / D) * (rho * u_avg^2 / 2);
fprintf('Basınç Kaybı: %.2f Pa\n', Delta_p);

% 3. Hız Profili
u_max = 2 * u_avg;          % Maksimum hız (m/s)
r = linspace(0, R, 100);    % Boru çapı boyunca noktalar (m)
u_r = u_max * (1 - (r.^2 / R^2)); % Hız profili

% 4. Basınç Dağılımı
x = linspace(0, L, 100);        % Boru uzunluğu boyunca noktalar (m)
p0 = input('Giriş basıncını girin (Pa): '); % Giriş basıncı (Pa)
p_x = p0 - Delta_p * (x / L);  % Basınç dağılımı

% Sonuçların Yazdırılması
fprintf('Maksimum Hız: %.2f m/s\n', u_max);
fprintf('Sürtünme Katsayısı: %.4f\n', f);
fprintf('Çıkış Basıncı: %.2f Pa\n', p_x(end));
```

Figure 24.
Matlab codes for straight pipe

```
% Kullanıcıdan Girdi Alma
D_in = input('Giriş borusu çapı (m): ');
D_out = input('Çıkış borusu çapı (m): ');
L_in = input('Giriş borusu uzunluğu (m): ');
L_out = input('Çıkış borusu uzunluğu (m): ');
theta = input('Çıkış açısı (derece): ');
u_in = input('Giriş hızını girin (m/s): ');
rho = input('Su yoğunluğunu girin (kg/m^3): ');
mu = input('Su dinamik viskozitesini girin (Pa·s): ');

% Boru Kesit Alanları
A_in = pi * (D_in / 2)^2;
A_out = pi * (D_out / 2)^2;

% 1. Reynolds Sayısı Hesabı
Re_in = (rho * u_in * D_in) / mu;
fprintf('Reynolds Sayısı (giriş): %.2f\n', Re_in);

% 2. Hız Dağılımı ve Çıkış Hızı Hesabı
u_out = u_in * (A_in / (2 * A_out));
fprintf('Çıkış Hızı: %.2f m/s\n', u_out);

% 3. Basınç Kaybı (Darcy-Weisbach)
if Re_in < 2300
    f_in = 64 / Re_in;
else
    f_in = 0.079 * Re_in^(-0.25);
end
Delta_p_in = f_in * (L_in / D_in) * (rho * u_in^2 / 2);
Delta_p_out = f_in * (L_out / D_out) * (rho * u_out^2 / 2);

fprintf('Giriş Borusu Basınç Kaybı: %.2f Pa\n', Delta_p_in);
fprintf('Çıkış Borusu Basınç Kaybı: %.2f Pa\n', Delta_p_out);

% Basınç Dağılımı
p0 = input('Giriş basıncını girin (Pa): ');
p_out = p0 - (Delta_p_in + Delta_p_out);
fprintf('Çıkış Basıncı: %.2f Pa\n', p_out);
```

Figure 25.
Matlab codes for bifurcation and trifurcation pipe

Conclusion

Straight pipes: As diameter increases (D=6,8,10 mm), velocity becomes more uniform, and turbulence decreases. Smaller diameters cause higher pressure drops due to friction, while larger diameters reduce resistance. Longer pipes (L=70,90 mm) slightly increase pressure drop, but larger diameters minimize this effect.

Bifurcation pipes: Larger diameters (D=6,8,10 mm) and bigger bifurcation angles (θ=50°,70°) lead to smoother and more uniform velocity distributions. Narrow pipes and sharper angles result in abrupt pressure drops, whereas larger diameters and smoother angles reduce pressure losses.

Trifurcation pipes: Increasing diameter (D=6,8,10 mm) spreads velocity uniformly, reducing central concentration and turbulence. Smaller diameters and shorter pipes exhibit the highest-pressure drops. Larger diameters reduce resistance, balancing flow and minimizing losses, even in longer pipes.

As a result, larger diameters (D=10 mm) and smoother transitions (θ=70°) increase flow uniformity, reduce turbulence and minimize pressure drops. Smaller diameters and sharper angles increase resistance and losses.

Peer-review: *Externally peer-reviewed.*

Author contributions:

A.K: Investigation, writing, literature search, analysis

İ.K : Supervision

Financial disclosure:

This research received no external funding.

Conflict of Interest: *The authors have no conflicts of interest to declare.*

References

Alharbi, A. Y., Pence, D. V., & Cullion, R. N. (2003). Fluid flow through microscale fractallike branching channel networks. *J. Fluids Eng., 125(6), 1051-1057.*

Bejan, A. (1997). Constructal tree network for fluid flow between a finite-size volume and one source or sink. *Revue generale de thermique, 36(8), 592-604.*

Blonski, S., Zaremba, D., Jachimek, M., Jakiela, S., Wacławczyk, T., & Korczyk, P. (2020). Impact of inertia and channel angles on flow distribution in microfluidic junctions. *Microfluidics and Nanofluidics, 24(2), 1-15.*

Chen, Y., & Cheng, P. (2002). Heat transfer and pressure drop in fractal tree-like microchannel nets. *International Journal of Heat and Mass Transfer, 45(13), 2643-2648.*

Colak, A.B. (2017). Tree shaped by bifurcation channels parallel and counter flow of heat exchanger heat transfer and flow investigation characteristics. [Master Thesis, Atatürk University, Institute of Science and Technology, Turkey]

Colak, A. B., Kotcioglu, I., & Khalaji, M. N. (2018). Tree Shaped in Channels Parallel and Counter Flow Through Heat Exchanger Heat Transfer and Flow Investigation of Characteristic. *Hittite Journal of Science and Engineering, 5, 33-49.*

Kotcioğlu, D. D. İ. (2017). Ağaç şekilli dal kanallı zıt ve paralel akışlı ısı değiştiricisinin ısı transferi ve akış karakteristiklerinin incelenmesi [Doctoral dissertation].

Lee, J. Y., & Lee, S. J. (2010). Murray's law and the bifurcation angle in the arterial microcirculation system and their application to the design of microfluidics. *Microfluidics and nanofluidics, 8(1), 85-95.*

Muwanga, R., Hassan, I., & Ghorab, M. (2008). Numerical investigation of a radial microchannel heat exchanger with varying cross-sectional channels. *Journal of thermophysics and heat transfer, 22(3), 321-332.*

Senn, S., & Poulikakos, D. (2004). Laminar mixing, heat transfer and pressure drop in tree-like microchannel nets and their application for thermal management in polymer electrolyte fuel cells. *Journal of Power Sources, 130(1-2), 178-191.*

Wang, X.-Q., Xu, P., Mujumdar, A. S., & Yap, C. (2010). Flow and thermal characteristics of offset branching network. *International Journal of Thermal Sciences*, 49(2), 272-280.